Structure and Bonding

DOI: 10.1002/anie.201207333

CuTe: Remarkable Bonding Features as a Consequence of a Charge Density Wave**

*Karoline Stolze, Anna Isaeva, Fabian Nitsche, Ulrich Burkhardt, Hannes Lichte, Daniel Wolf, and Thomas Doert**

Materials with one-dimensional properties are both a fascinating topic and a challenging task in solid-state chemistry. Among these materials, compounds with equidistant linear one-atomic chains are often discussed as they can show Peierls-type instabilities.[1] In crystalline solids that consist of more than one structural building unit, however, the electronics, and thus the bonding situation, can be more complicated.[2] CuTe, also known as mineral vulcanite, is one of the rare binary phases in which equidistant linear chains of a main-group element (tellurium in this case) were found.[3] The Te chains run above and below a puckered copper layer so that each copper atom has a distorted tetrahedral environment (Figure 1). No manifestation of a Peierls-like distortion of the Te chains has previously been found for this compound, and metallic conductivity was determined experimentally.[4,5]

In recent X-ray diffraction experiments on single crystals, however, we discovered that the structure of CuTe indeed exhibits a charge density wave (CDW)-type modulation. The modulation leads to a significantly different bonding situation as compared to the average or non-modulated structure.

The diffraction images of CuTe crystals at ambient temperature show previously unrecognized weak satellite reflections beneath the main reflections of the orthorhombic basic unit cell of $a = 3.151(1)$ Å, $b = 4.089(1)$ Å, and $c = 6.950(1)$ Å (Supporting Information, Figures S4 and S5). A model of the modulated structure has been developed in the (3+1)-dimensional superspace group $Pmmn(\alpha 0 {}^1/_2)000$ with a modulation wave vector $\mathbf{q} = (\alpha 0 {}^1/_2)$ and $\alpha = 0.40(1)$ using the superspace approach.[6] The modulation primarily influences the Te–Te distances in the Te chains, which were found to vary from 305 pm to 326 pm at $T = 295$ K (average structure: 315 pm). As a result, units of two or three tellurium atoms with shorter distances alternate with single tellurium atoms along [100] (Figure 2). Even though the shorter Te–Te distances exceed the sum of the covalent radii of 276 pm,[7] attractive interactions must be considered, as bonding distances between 290 pm and 310 pm are a well-known feature in polytellurides, and especially in the so-called non-classical polytellurides with multicenter bonds.[2,8]

The modulation of the Te position also forces a distortion of the corrugated Cu layers, leading to a slight deflection of the Cu atoms along [001] (Supporting Information, Table S3). The Cu–Cu distances, however, vary only slightly (265–268 pm at $T = 295$ K; average structure 266 pm).

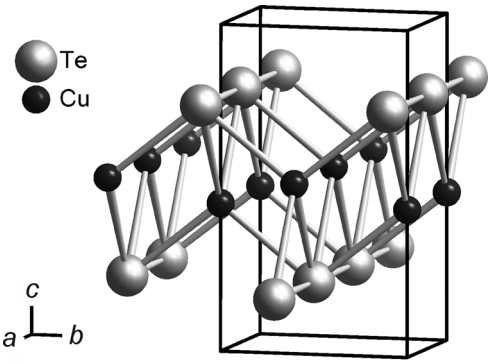

Figure 1. Crystal structure of CuTe.[3] The shortest interatomic Cu–Te and Te–Te distances indicated as solid lines.

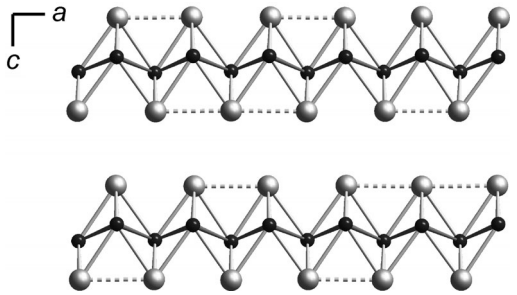

Figure 2. Section of the modulated structure of CuTe. The shortest Cu–Cu, Cu–Te, and Te–Te distances indicated as solid and dashed lines, respectively.

[*] K. Stolze, Dr. A. Isaeva, F. Nitsche, Prof. Dr. T. Doert
Fachrichtung Chemie und Lebensmittelchemie
Technische Universität Dresden
01062 Dresden (Germany)
E-mail: thomas.doert@chemie.tu-dresden.de
Dr. U. Burkhardt
Max Planck Institut für Chemische Physik fester Stoffe
Nöthnitzer Strasse 40, 01187 Dresden (Germany)
Prof. Dr. H. Lichte, Dr. D. Wolf
Triebenberg Labor & Institut für Strukturphysik
Technische Universität Dresden
01062 Dresden (Germany)

[**] We thank Dr. G. Auffermann, Max Planck Institute for Chemical Physics of Solids for chemical analyses, Dr. M. Tolkien for support at the synchrotron beamline D3 (HAYSLAB/DESY), and the ZIH TU Dresden for the computational facilities provided within the project "Chemical Bonding Analysis of Novel Inorganic Compounds with Real-Space Indicators".

Supporting information for this article is available on the WWW under http://dx.doi.org/10.1002/anie.201207333.

The modulation vanishes at slightly elevated temperatures. At $T \geq 350$ K no satellite intensities with $I > 3\sigma(I)$ are detectable. The non-modulated high-temperature phase corresponds to Pertlik's model of the average structure.[3] Upon cooling the satellite intensities, and thus the impacts of the modulation, increase: The shortest Te–Te contacts range from 305 pm to 315 pm at $T = 295$ K and from 295 pm to 308 pm at $T = 20$ K. The modulation wave vector itself does not change in this temperature interval.

HRTEM studies reveal that the layers of CuTe are perfectly ordered along the c axis (Figure 3). The dark columns correspond to rows of atoms while the bright spots represent cavities. The Fourier transform shown in the inset

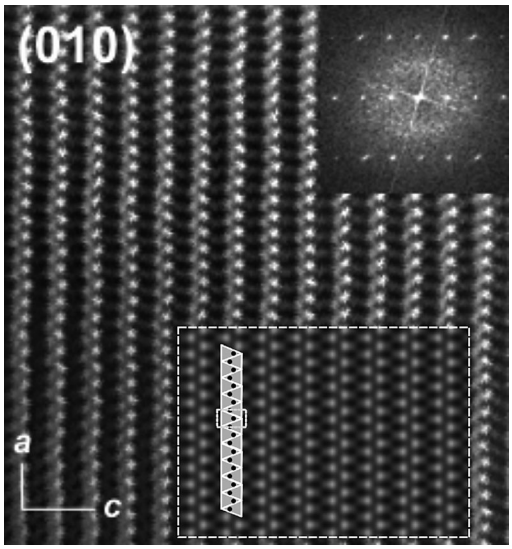

Figure 3. Theoretical (dashed white outline) and experimental (010) zone HRTEM images of CuTe. The theoretical contrast compares well to the JEMS simulation with a defocus value of −100 nm, and appears to be insensitive to the thickness and fits to a range between 2.4 and 8.6 nm. The corresponding Fourier transform is shown as an inset. The dotted white line outlines the unit cell. An overlaid atomic row depicts black Cu circles in gray Te_4 tetrahedra.

(upper right in Figure 3) agrees well with the experimental electron diffraction (ED) pattern of the [010]* zone (Supporting Information, Figure S3). No satellites could be recorded, as the extensive illumination leads to local sample heating and to quickly vanishing satellite intensities. The ED pattern thus corresponds to the average CuTe structure. No evidence for additional Cu positions was found, in accordance with chemical analyses and X-ray diffraction results.

How does the modulation now affect the chemical bonding in CuTe? Apparently, a simplified electron count based on a Zintl–Klemm approach is not straightforward, even for the average structure. There is evidence for copper in an oxidation state close to +1 from X-ray absorption data consistent with its distorted tetrahedral coordination environment.[9] However, tellurium should then either be Te^-, and thus a classical candidate for a Peierls-type instability, or it should adopt an even lower oxidation state, in accordance with its metallic conductivity, which can be rationalized by the formula $Cu^+Te^{1-x}(e^-)_x$. A previous extended Hückel consideration based on the average structure of CuTe describes the bonding features mainly by focusing on the molecular orbitals of the (more or less) tetrahedral $CuTe_4$ units.[4] This approach, however, is too narrowly considered, especially for the modulated structure (see below).

Periodic band-structure calculations[10] demonstrate no significant differences in the band dispersions between average and modulated CuTe structures (Supporting Information, Figure S8). However, surprisingly high atomic charges +1.9 for Cu and −1.9 for Te have been computed in the former using the ELIBON concept (electron-localizability-indicator-based oxidation numbers[11]). The modulation is found to considerably rectify this unfavorable charge distribution, which can be regarded as a major part of the driving force: The partial oxidation in the tellurium sublattice towards Te_2^{2-} and Te_3^{2-} anions and the concomitant increased Cu–Cu interactions reduce the charges to +1.4 for Cu and −1.4 for Te (see the Supporting Information, Table S8, for the details of charge distribution scenarios).

A closer look at the bonding situations, established from the real-space topological analysis of the ELI-D field (electron localizability indicator),[10d] reveals further decisive differences between the average and modulated structures. In the former, covalent bonding interactions between Cu and Te, manifesting itself as ELI-D basins populated by 0.9 electrons (Figure 4, left), are dominant. No direct interactions between

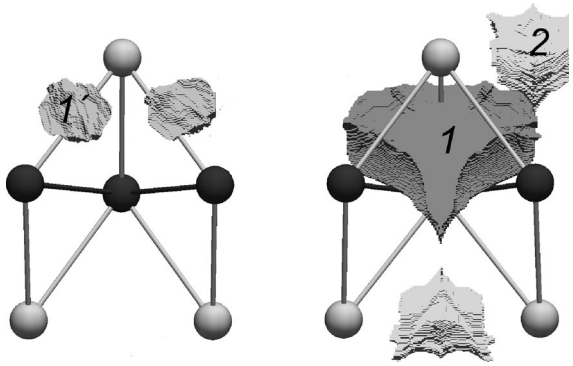

Figure 4. Left: Bonding features (ELI-D basins) in the average structure of CuTe. **1′**: Te (60%) + Cu (40%) populated by 0.9 electrons. Right: Bonding features in the modulated structure of CuTe. **1**: Te (62%) + 3 Cu atoms (38%) populated by 1.8 electrons; **2**: Te1 (51%) + Te2 (49%) populated by 0.45 electrons.

Te atoms in the linear chain are observed. For the modulated structure, the bonding between those Te atoms having the shorter interatomic distances (295–308 pm at $T = 20$ K) becomes evident and the corresponding ELI-D basins now host about 0.45 electrons (Figure 4, right). Moreover, the Cu–Te bonding is also affected and turns out to be delocalized among three Cu and one Te atom on top, all of them constituting a joint bonding ELI-D basin bearing 1.8 electrons. This intensified mutual interaction is also evident from the increased bond strengths in the modulated structure compared to the average one indicated by the integrated crystal orbital Hamilton population values (−ICOHP;

numerical values given in eV/cell per contact): 0.49 vs. 0.30 for Cu–Cu contacts, 1.61 vs. 1.31 for Cu–Te contacts. The Te–Te interactions increase from 0.31 (linear chain) to 0.40 for Te_3^{2-} and 0.73 for Te_2^{2-} units in the modulated phase (Supporting Information, Figure S10).

The modulation, thus, not only increases the Te–Te interactions considerably, but leads to multicenter Cu–Te interactions that supersede the classical two-center bonds, a situation habitually found in metal-rich compounds. Evidence for the substantial multicenter Cu–Cu interactions in the *ab* plane, accompanying the Cu–Te interactions, can also be found (Supporting Information, Figure S11). Owing to the degeneration in the Te chains, these interactions provide the only continuous electron conduction path as evidenced also by the increased Cu contribution to the density-of-states (DOS) near the Fermi level. Whereas for the average structure metallic conductivity is mainly provided by Te $5p_x$ states,[4] the modulated structure also demonstrates profound contribution of Cu 3d states against the background of prevalent Te p states at the Fermi level (Supporting Information, Figure S9). The positional modulation also reduces the DOS at the Fermi level, approximately by a factor of two. It is, however, not strong enough to render CuTe a semiconductor as would be expected for a true one-dimensional Peierls system.

In summary, a CDW type modulation has been found in CuTe that can be understood as a result of a competition for electrons among copper and tellurium. The electronic balance is attained by the formation di- and tritelluride anions together with increased multicenter Cu–Te and Cu–Cu interactions. Modulated CuTe thus combines typical bonding features of polyanionic as well as metal-rich compounds.

Experimental Section

Synthesis: All manipulations with the starting reagents were carried out under argon (Air Liquide, 99.999%). Copper (Chempur, powder, 99.95%, reduced at 670 K with H_2, (Air Liquide, 99.99%)), and tellurium (Fluka, chunks, 99.999%, reduced at 670 K with H_2) were mixed in a molar ratio of 1:1 and ground. Approximately 500 mg of the mixture was loaded into a silica ampoule. The ampoule was filled with 6 mL ethylenediamine (Merck, analytic grade) to an approximate filling degree of 50% and sealed under dynamic vacuum upon cooling the suspension with liquid nitrogen. For safety reasons, the ampoule was placed in a lockable steel tube. The sample was annealed at 470 K, regularly homogenized by shaking and after 24 days cooled to room temperature within one day. The solvent was decanted and the product was washed with water and ethanol. Air-stable, gold-colored, metallic lustrous crystals of CuTe were obtained (Supporting Information, Figure S2).

Analyses: Phase purity of the reaction products was checked by X-ray powder diffraction on a XPert PRO diffractometer (PANalytical) with Cu$K\alpha_1$ radiation ($\lambda = 154.056$ pm), Ge monochromator, Bragg–Brentano setup). Data were analyzed with the WinXPow program package.[12] The copper and tellurium content of a single phase sample was probed via ICP-OES analysis and resulted in a composition of $Cu_{1.00(1)}Te_{1.00(1)}$. Energy dispersive X-ray analyses (EDX, Philips XL30 scanning electron microscope with a Phoenix V 5.29 analytic unit, EDAX) and wavelength dispersive X-ray analyses (WDX, Cameca SX100 microprobe, Cu and ZnTe standard) analyses were performed on cleaved and polished faces of several crystals of a sample with a Cu/Te starting ratio of 1:1. EDX results: $Cu_{1.01(1)}Te_{1.00(1)}$, PAP-matrix corrected WDX results: $Cu_{1.05(2)}Te_{1.00(2)}$.

Single-crystal X-ray diffraction: CuTe, Orthorhombic, (3 + 1)D superspace group $Pmmn(\alpha 0 \frac{1}{2})000$[13] with $\alpha = 0.400(1)$; $a = 315.12(2)$, $b = 408.91(2)$, $c = 694.96(4)$ pm; $V = 89.55(1) \times 10^6$ pm^3; $Z = 2$; $\rho_{calcd} = 7.09$ g cm^{-3}; Apex-II CCD diffractometer (Bruker-AXS), Mo-$K\alpha$ radiation ($\lambda = 71.073$ pm), $T = 295$ K; multiscan absorption correction,[14] μ(Mo-$K\alpha$) = 27.6 mm^{-1}; 5148 measured, 686 unique reflections (second-order satellites excluded from refinement owing to very weak intensities), $R_{int} = 0.022$, $R_\sigma = 0.021$; structure solution by charge flipping,[15] refinements performed with JANA2006,[16] one harmonic modulation wave for the positional modulation of Te and Cu atoms and for their anisotropic displacement parameters, (Supporting Information, Table S2). Residuals: For all reflections: R_1 ($413 F_o > 3\sigma(F_o)$) = 0.020, R_1(all F_o) = 0.038, wR_2(all F_o^2) = 0.050; $GooF = 1.28$; residual electron density: −0.91 to +0.82 e × 10^{-6} pm^{-3}. The results of the data collection performed at $T = 20$ K are listed in the Supporting Information, Tables S5–S7.

The temperature dependence of the modulation was checked on a Apex-II CCD diffractometer (see above) and at the D3 synchrotron beamline at HASYLAB (Huber four-circle diffractometer, Mar CCD 165, Oxford diffraction Helijet). Apart from the thermal expansion, the same diffraction images were observed in the interval $20 \le T \le 300$ K. At $T \ge 350$ K, no satellite intensities could be detected.

Further details on the crystal structure investigation(s) may be obtained from the Fachinformationszentrum Karlsruhe, 76344 Eggenstein-Leopoldshafen, Germany (fax: (+49) 7247-808-666; e-mail: crysdata@fiz-karlsruhe.de), on quoting the depository numbers CSD-424929 (295 K) and CSD-424930 (20 K).

Electron microscopy and diffraction: Samples were prepared by grinding phase-pure polycrystalline samples in ethanol and deposing fragments on a holey carbon grid. High-resolution transmission electron microscopy (HRTEM) and selected area electron diffraction (SAED) studies were performed on a FEI Tecnai F20 with Cs-correction operating at 200 kV. For image acquisition, a 1k Slow-Scan CCD-Camera (Gatan) was used. Image simulations were carried out with the JEMS software.[17]

Quantum-chemical calculations: Scalar-relativistic DFT calculations were performed by the full-potential LAPW method[10a] within the generalized gradient approximation (GGA) employed for the exchange-correlation functional.[10b] Chemical bonding was characterized through the topological analysis of the electron density[10c] and of the electron localizability indicator (ELI-D)[10d] for the local density approximation. The COHP were calculated using the TB-LMTO-ASA package.[10e]

Received: September 11, 2012
Published online: November 23, 2012

Keywords: charge density waves · chemical bonding · copper telluride · modulated structure · polytellurides

[1] R. E. Peierls, *Quantum Theory of Solids*, Oxford University Press, London, **1955**, pp. 101–114.
[2] a) K. Stöwe, *Z. Anorg. Allg. Chem.* **1996**, *622*, 1423; b) K. Stöwe, F. R. Wagner, *J. Solid State Chem.* **1998**, *138*, 160; c) K. Stöwe, *J. Solid State Chem.* **2000**, *149*, 123.
[3] a) E. N. Cameron, I. M. Threadgold, *Am. Mineral.* **1961**, *46*, 258; b) F. Pertlik, *Miner. Petrol.* **2001**, *71*, 149.
[4] S. Seong, T. A. Albright, X. Zhang, M. Kanatzidis, *J. Am. Chem. Soc.* **1994**, *116*, 7287.
[5] K. Neyvasagam, N. Soundararajan, Ajaysoni, G. S. Okram, V. Ganesan, *Phys. Status Solidi B* **2008**, *245*, 77.
[6] a) A. Janner, T. Janssen, *Phys. Rev. B* **1977**, *15*, 643; b) S. van Smaalen, *Incommensurate Crystallography*, Oxford University Press, Oxford, **2007**.

[7] B. Cordero, V. Gómez, A. E. Platero-Prats, M. Revés, J. Echeverría, E. Cremades, F. Barragán, S. Alvarez, *Dalton Trans.* **2008**, 2832.
[8] a) P. Böttcher, U. Kretschmann, *Z. Anorg. Allg. Chem.* **1982**, *491*, 39; b) F. Klaiber, W. Petter, F. Hulliger, *J. Solid State Chem.* **1983**, *46*, 112; c) W. S. Sheldrick, M. Wachhold, *Angew. Chem.* **1995**, *107*, 490; d) Th. Doert, R. Cardoso-Gil, P. Böttcher, *Z. Anorg. Allg. Chem.* **1999**, *625*, 2160; e) A. Assoud, S. Derakhshan, N. Soheilnia, H. Kleinke, *Chem. Mater.* **2004**, *16*, 4193; f) J.-Q. Wang, S. D. Hoffmann, T. F. Fässler, *Z. Anorg. Allg. Chem.* **2008**, *634*, 2917; g) W. S: Sheldrick,. *Z. Anorg. Allg. Chem.* **2012**, in press, DOI: 10.1002/zaac.201200241.
[9] M. K. Bahl, *J. Phys. C* **1975**, *8*, 4107.
[10] a) ELK, All-electron full-potential linearized augmented-plane wave code (http://elk.sourceforge.net, accessed on 2011-11-23); b) J. P. Perdew, Y. Wang, *Phys. Rev. B* **1992**, *45*, 1324; c) R. F. W. Bader, *Atoms in Molecules*, Oxford Univ. Press, Oxford, **1990**; d) M. Kohout, *Faraday Discuss.* **2007**, *135*, 43; M. Kohout, DGrid, Version 4.6e, Radebeul, **2011**; e) F. Boucher, O. Jepsen, O. K. Andersen, *The Supplement to the TB-LMTO-ASA*, Version 4.7c, **1997**.
[11] I. Veremchuk, T. Mori, Yu. Prots, W. Schnelle, A. Leithe-Jasper, M. Kohout, Yu. Grin, *J. Solid State Chem.* **2008**, *181*, 1983.
[12] Win XPOW 2.25, Stoe & Cie GmbH, Darmstadt, **2011**.
[13] a) P. M. de Wolff, T. Janssen, A. Janner, *Acta Crystallogr. Sect. A* **1981**, *37*, 625; b) A. Yamamoto, T. Janssen, A. Janner, P. M. de Wolff, *Acta Crystallogr. Sect. A* **1985**, *41*, 528.
[14] SADABS, Bruker Axs, Karlsruhe, **2008**.
[15] a) G. Oszlányi, A. Sütő, *Acta Crystallogr. Sect. A* **2004**, *60*, 134; b) G. Oszlányi, A. Sütő, *Acta Crystallogr. Sect. A* **2008**, *64*, 123.
[16] JANA2006, The Crystallographic Computing System, V. Petricek, M. Dusek, L. Palatinus, Prague, **2011**.
[17] JEMS, version 3.7624U2012, http://cimewww.epfl.ch/people/stadelmann/jemsv3_7624u2012.htm (accessed on 2012-03-06).

